

Functional Evaluation of Submerged Bricks Porosity Based on the Conjugal Influence of Post-Fired Volume Shrinkage and Water Absorption Level

¹C.I. Nwoye, ²N.M. Okelekwe, ³M. Joseph, ⁴O.M. Okoronkwo and ³G.O. Ewah

¹Department of Metallurgical and Materials Engineering,
Nnamdi Azikiwe University, Awka, Nigeria

²Department of Vocational, Technical and Skills Development,
National Board for Technical Education, Kaduna, Nigeria

³Department of Metallurgical Engineering Technology,
Akanu Ibiam Federal Polytechnic, Afikpo, Ebonyi State, Nigeria

⁴Setraco Nigeria Limited, Amasiri Quarry, Ebonyi State, Nigeria

Abstract: A functional evaluation of submerged bricks apparent porosity (AP) was carried out based on the conjugal influence of post-fired volume shrinkage (PFVS) and water absorption level (WAL). Mined clay sample was prepared and processed, following a well detailed step-wise route. Empirical Analysis of the AP of the produced bricks while serving under submerged condition was carried out using a two-factorial model expressed as $\delta = 102.3089 - 0.9501 \xi - 2.5076 \vartheta$. The validity of the derived model was rooted in the core expression $\delta - 102.3089 = -0.9501 \xi - 2.5076 \vartheta$ where both side of the expression are correspondingly approximately equal. Results evaluated from both experiment and model prediction indicated increase in AP as PFVS decreases, culminating to increase in WAL. Generated results indicated that the correlations between AP, WAL and PFVS and the standard error incurred in predicting AP for each value of the PFVS & WAL considered, as obtained from experiment, derived model and regression model were all > 0.95 as well as 0.0659, 0.0668 and 0.0031 & 0.0027, 0.2111 and 0.0637 % respectively. The maximum deviation of the model-predicted AP (from experimental results) was less than 6%. This translated into over 94% operational confidence for the derived model as well as over 0.94 effective coefficients for the functional relationship between AP, WAL and PFVS of the submerged bricks.

Key words: Functional Evaluation - Apparent Porosity - Post-Fired Volume Shrinkage - Water Absorption - Submerged Bricks

INTRODUCTION

The need to produce building materials such as bricks with high post-fired volume shrinkage and low water absorption capacity (low porosity) has been considered a major factor towards eliminating abrupt failures resulting from the incessant collapse of buildings in the riverine areas especially in Nigeria, and also in other environments there is always stagnation of water around buildings (as a result of flood).

It has been reported [1] that the strength of ceramics is adversely affected by pores on one hand by acting as stress concentrators and on the other reducing the cross-sectional area over which load is applied.

It is strongly believed that bricks for building constructions need have good structural stability through improvements in its chemical, physical and mechanical properties if enhanced durability level is to be achieved.

Corresponding Author: C.I. Nwoye, Chemical Systems and Data Research Laboratory, Department of Metallurgical and Materials Engineering, Nnamdi Azikiwe University, Awka, Nigeria.
E-mail: nwoyennike@gmail.com

Investigations [2-7] into the formability of ceramics have shown that it can be moulded into different shapes and configurations for different uses depending on the forming techniques employed.

Studies [1, 8, 9, 10] on clay shrinkage during drying have shown that porosity influences the swelling and shrinkage behaviour of clay products of different geometry. Research [9] shows that drying occurs in three stages; increasing rate, constant and decreasing rate. The scientist posited that during the increasing rate; evaporation rate is higher than evaporating surface hence more water is lost. At constant rate, the evaporation rate and evaporation surface are constant. The report explicitly indicated that shrinkage bnve occurs at this stage.

Results from a similar study [10] also agreed firmly that at this stage, free water is removed between the particles, and so the inter-particle separation decreases, resulting in shrinkage. The researcher further posited that during the decreasing rate, particles make contacts as water is removed, causing shrinkage to cease.

Fine particles have been reported [8] to shrink more, exhibit excellent mechanical properties and also denser than larger ones. Results from the report evaluating the relationship between particle size and size distribution with linear drying shrinkage revealed that firing shrinkage and apparent porosity have no visible relationship with particle size and linear drying shrinkage. The researcher therefore concluded based on these results that the finer the particle size, the lesser the apparent porosity and greater the bulk density.

An empirical relationship [11] between the volume shrinkage and the initial air-drying of wet clay has been successfully derived [11]. The derived model;

$$\theta = \gamma^3 - 3\gamma^2 + 3\gamma \quad (1)$$

calculates the volume shrinkage θ when the value of dried shrinkage γ , experienced during air-drying of wet clays is known. The model is third-order polynomial in nature. Olokoro clay was characterized with the highest shrinkage during the air drying condition, followed by Ukpor clay while Otamiri clay has the lowest shrinkage. Volume shrinkage was discovered to increase with increase in dried shrinkage until maximum volume shrinkage was reached, hence a direct relationship.

A successful attempt [12] was also made to derive an expression for the Overall volume shrinkage in molded clay products (from initial air-drying stage to completion of firing at a temperature of 1200°C). The model was expressed as;

$$S_T = \alpha^3 + \gamma^3 - 3(\alpha^2 + \gamma^2) + 3(\alpha + \gamma) \quad (2)$$

Evaluated results indicated proximate agreement on comparing results of the overall volume shrinkage predicted by the model and those generated from the conventional equations. The results indicated that overall volume shrinkage depended on direct values of the dried γ and fired shrinkage α for its precision. Overall volume shrinkage increased with increase in dried and fired shrinkages until overall volume shrinkage reaches maximum.

Two-factorial empirical analysis of Post-Fired Volume Shrinkage (PFVS) was carried out [13] based on its apparent porosity (AP) and water absorption capacity (WAC). The analysis was carried out using a model expressed as;

$$\vartheta = -0.3988 \wp - 0.3789 \xi + 39.256 \quad (3)$$

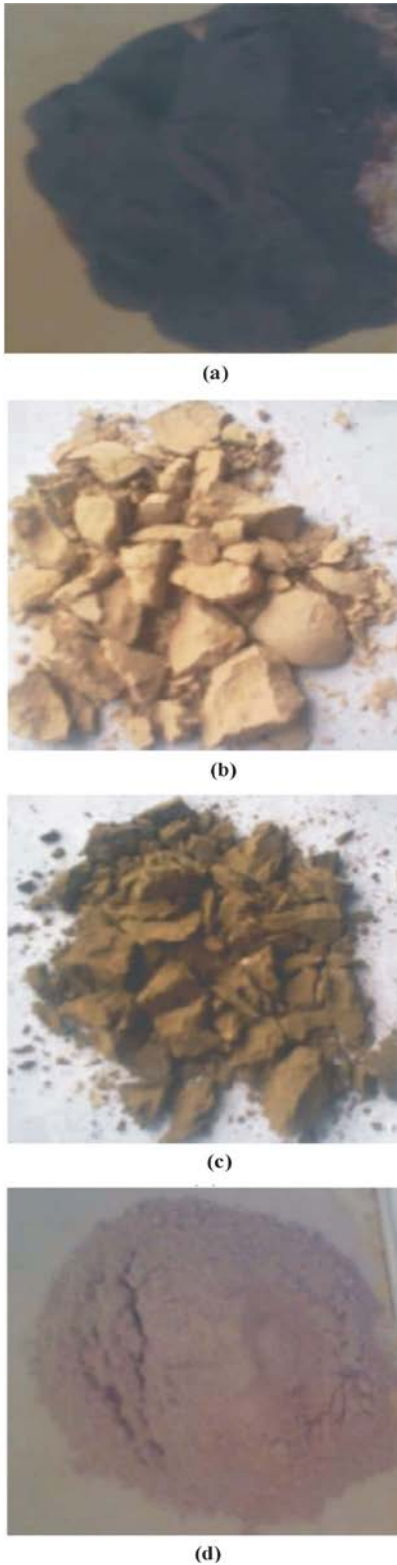
where ϑ = PFVS, \wp = AP and ξ = WAC.

The maximum deviation of the model-predicted water absorption (from experimental results) was less than 5.57%. This translated into over 94% operational confidence for the derived model as well as over 0.94 effective response coefficients of WAC and apparent porosity to PFVS of the bricks. Furthermore, the correlations between PFVS and WAC & apparent porosity as obtained from experiment, derived model and regression model were all > 0.97 .

The present work aims at functional evaluation of submerged bricks apparent porosity based on the conjugal influence of post-fired volume shrinkage and water absorption level.

MATERIALS AND METHODS

The materials used for this research work includes Olokoro Clay mined at Umuahia, Abia State and Bentonite obtained from Bridge Head Market, Onitsha, Anambra state, Nigeria. The chemical composition of the clay used is shown in Table 1.



Figs. 1: (a) Olokoro clay (as mined) (b) Dried Olokoro clay (c) Dried Olokoro clay mixed with Bentonite (d) Bentonite powder

Clay Sizing and Moulding: An assembly of sieves having opening as 100, 300 and 1000 μm in ascending order was used for size analysis of the clay. The sieve assembly was placed on a mechanical sieve shaker and power supply switched on. The set-up was allowed to function for 4 minutes. Particle sizes lesser than 100 μm were designated as fine particle size (A), those at 100 μm were designated as less finer (B), those lesser than 300 μm were designated as medium particle size (C), those at 300 μm were taken as enhanced medium particle size (D) while particle size within range 300-1000 μm were designated as coarse particle size (E). The sieving process was repeated severally until the quantity of clay required for the moulding process was available. Hundred grams (100g) of the sieved clay sample and 10g of bentonite powder were weighed out and thoroughly mixed. To increase the plasticity and strength of the clay material during firing, bentonite powder was added. Six percent (6%) of total weight (clay and Bentonite) of water was added and it was then mixed until complete homogeneity was achieved. The mixed samples were poured into the rectangular metal mould of internal dimension 50 x 18 x 10 mm. The green samples were marked immediately after moulding with two parallel lines (along the length) 70 mm apart. The distance between these lines is L.

Air Drying: Following the moulding process, the specimens were carefully placed in a plastic tray and kept outside the laboratory to lose some water and become strengthened. The reason for air drying includes (1) to prevent the samples from being defective as a result of evaporation during oven drying and firing (2) to give the specimens adequate strength during oven drying and firing.

Oven Drying and Firing: After air-drying an electrically heated oven of internal dimension 500 x 500mm was used in the drying operation. The oven was sourced from Erosion Research Center of the Federal University of Technology, Owerri (FUTO). Each set of the specimens was dried at a temperature of 125°C for 1hr, after which their respective weights were measured. The clay samples were then charged into an electric kiln and heated at a lower temperature 125°C, after which the temperature was increased and fired at 1200°C for 48 hrs. The samples were cooled in the furnace for 48hrs after firing. The distance between the two parallel lines was determined after oven drying L_1 and firing L_2 .

Determination of post-fired volume shrinkage, apparent porosity and water absorption

Post-fired volume shrinkage V , was calculated using the formular:

$$V = 1 - [(1 - (L - L_2)/L)^3] \times 100 \quad (4)$$

where

L = Original length (mm);

L_1 = Dry length (mm);

L_2 = Fired length (mm)

Apparent porosity and water absorption level were determined using the conventional standard technique. [14]

RESULTS AND DISCUSSION

Result of chemical analysis of Olokoro clay shown in Table 1 shows that Na_2O (in the clay) is the poorest constituent while SiO_2 and then Al_2O_3 mostly constituted the clay.

Table 1: Chemical composition of Olokoro clays

Constituents	(%)
Al_2O_3	29.10
SiO_2	45.44
MgO	0.75
Na_2O	0.05
K_2O	0.09
CaO	1.26
Fe_2O_3	7.93
LOI	11.90

Table 2: Variation of WAL, PFVS and AP

(ϑ)	(\aleph)	(ζ)	Grain size (μm)
25.63	21.90	16.68	< 100
25.52	22.01	16.79	100
25.07	22.44	17.25	< 300
24.97	22.46	17.27	300
24.82	22.48	17.29	300-1000

Water absorption decreases (as shown in Table 2) with decreasing apparent porosity and increasing post-fired volume shrinkage. This was so because during firing, water present in the clay was significantly removed, and simultaneously aiding enhanced decrease in the inter-particle spacing, leading to increased post-fired volume shrinkage in accordance with past findings [10].

It is important to note that a good knowledge of the empirical relationship between the quantity of water absorbed (by the brick in submerged condition) and the post-fired volume shrinkage & apparent porosity gives a structural engineer an idea of what to expect in terms

of water absorption of the bricks (when used for building in easily flood environment) for any choice of clay particle size inculcated in producing bricks for building.

Increase in the clay grain size (as in Table 2) results to increase in the water absorption of the produced bricks due to increase in the apparent porosity and decrease in the post-fired volume shrinkage. This is also in line with past research [8].

Model Formulation: Results generated from this research work were used for the model formulation. Computational analysis of the data shown in Table 2, gave rise to Table 3 which indicate that;

$$\aleph - H \approx - N \xi - K \vartheta \quad (5)$$

Introducing the values of H , N and K , into equation (5) reduces it to;

$$\aleph - 102.3089 = - 0.9501 \xi - 2.5076 \vartheta \quad (6)$$

$$\aleph = 102.3089 - 0.9501 \xi - 2.5076 \vartheta \quad (7)$$

where

(ϑ) = Post fired volume shrinkage (%)

(\aleph) = Apparent porosity (%)

(ζ) = Water absorption (%)

$H = 102.3089$, $N = 0.9501$, and $K = 2.5076$ These are empirical constants (determined using C-NIKBRAN [15])

Boundary and Initial Condition: Consider a rectangular shaped clay product of length 49mm, width 17mm, and breadth 9mm exposed to drying in the oven while it was in slight wet condition and then fired in the furnace. Initially, atmospheric levels of oxygen are assumed. Atmospheric pressure was assumed to be acting on the clay samples during the drying process (since the furnace is not air-tight). The sizes of clay particles used were < 100, 100-300 and 300-1000 μm while weights of clay and binder (bentonite) used (for each rectangular product) were 100g and 10g respectively. Quantity of water used for mixing was 6% (of total weight). Oven drying and firing temperatures used were 125 and 1200 $^{\circ}C$ for 1and 48 hrs respectively. Area of evaporating surface was 833mm². Cooling time for samples was 48 hrs.

The boundary conditions are: atmospheric levels of oxygen at the top and bottom of the clay samples since they are dried under the atmospheric condition. No external force due to compression or tension was

applied to the drying clays. The sides of the particles and the rectangular shaped clay products are taken to be symmetries.

Model Validation:

Table 3: Variation of $\xi - 102.3089 = -0.9501 \xi - 2.5076 \vartheta$

$\xi - 102.3089$	$-0.9501 \xi - 2.5076 \vartheta$
-80.1189	-80.1175
-79.9489	-79.9462
-79.2589	-79.2547
-79.0189	-79.0230
-78.6689	-78.6658

Equation (7) is the derived model. The validity of the model is strongly rooted on equation (6) where both sides of the equation are correspondingly approximately equal. Table 3 also agrees with equation (6) following the values of $\xi - 102.3089 = -0.9501 \xi - 2.5076 \vartheta$ evaluated from the experimental results in Table 2.

Furthermore, the derived model was validated by comparing the model-predicted water absorption and that obtained from the experiment. This was done using the 4th Degree Model Validity Test Techniques (4th DMVTT); statistical graphical, and deviational analysis.

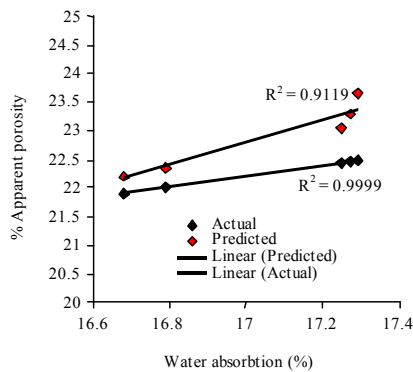


Fig.2: Coefficient of determination between apparent porosity and water absorption level as obtained from actual and predicted results

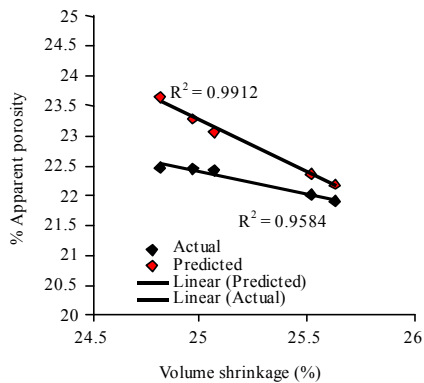


Fig.3: Coefficient of determination between apparent porosity and volume shrinkage as obtained from actual and predicted result

Statistical Analysis

Standard Error (STEYX): The standard error incurred in predicting the model-based AP relative to values of the actual results is 0.21%. The standard error was evaluated using Microsoft Excel version 2003.

Correlation (CORREL): The correlation coefficient between AP and PFVS &WAL were evaluated from the results of the derived model and experiment, considering the coefficient of determination R^2 from Figs. 2 and 3. The evaluation was done using Microsoft Excel version 2003.

$$R = \sqrt{R^2} \tag{8}$$

The evaluated correlations are shown in Tables 4 and 5. These evaluated results indicate that the derived model predictions are significantly reliable and hence valid considering its proximate agreement with results from actual experiment.

Table 4: Comparison of the correlations evaluated from derived model predicted and ExD results based on WAL

Analysis	Based on WAL	
	ExD	D-Model
CORREL	0.9999	0.9549

Table 5: Comparison of the correlation evaluated from derived model-predicted ExD based on PFVS

Analysis	Based on PFVS	
	ExD	D-Model
CORREL	0.9790	0.9956

Graphical Analysis: Comparative graphical analysis of Figs. 4 and 5 show very close alignment of the curves from the experimental (ExD) and model-predicted (MoD) apparent porosity.

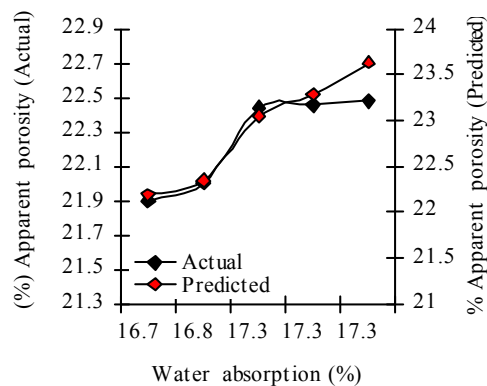


Fig.4: Comparison of apparent porosity (relative to WAL) as obtained from actual and model-predicted results

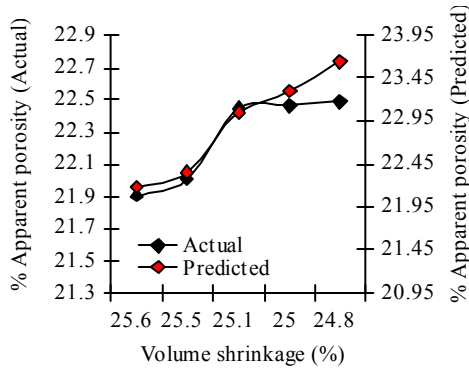


Fig.5: Comparison of apparent porosity (relative to PFVS) as obtained from actual and model-predicted result.

Furthermore, the degree of alignment of these curves is indicative of the proximate agreement between both experimental and model-predicted apparent porosity.

Comparison of Derived Model with Standard Model: The validity of the derived model was also verified through application of the regression model (Reg) (Least Square Method using Excel version 2003) in predicting the trend of the experimental results.

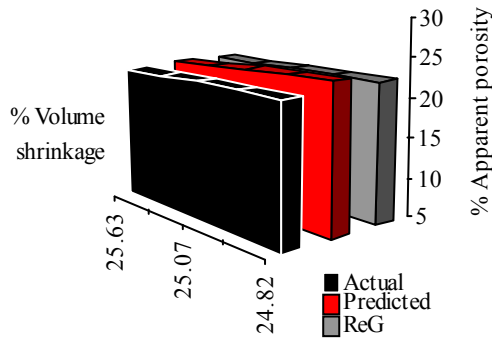


Fig.6: 3-D Effects comparison of apparent porosities (relative to PFVS) as obtained from actual, derived model and regression model

Comparative analysis of Figs. 6 and 7 shows very close alignment of curves and areas covered by apparent porosity, which precisely translated into significantly similar trend of data point's distribution for experimental (ExD), derived model (MoD) and regression model-predicted (ReG) results of apparent porosity.

Also, the calculated correlations (from Figs. 6 and 7) between AP and PFVS & WAL for results obtained from regression model gave 0.9999 & 0.9790 respectively. These values are in proximate agreement with both experimental and derived model-predicted results. The standard errors

incurred in predicting regression-based AP relative to the actual values is 0.06%.

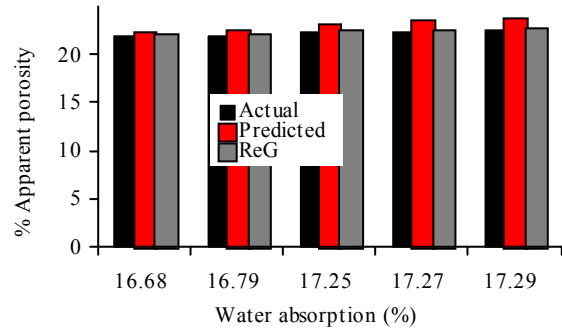


Fig.7: Comparison of apparent porosity (relative to WAL) as obtained from experiment, derived model and regression model

Deviational Analysis: The deviation D_v , of model-predicted apparent porosity from the corresponding experimental result was given by;

$$D_v = \left(\frac{\delta_{MoD} - \delta_{ExD}}{\delta_{ExD}} \right) \times 100 \quad (9)$$

where

δ_{ExD} and δ_{MoD} are apparent porosities obtained from experiment and derived model respectively.

Critical analysis of the apparent porosities obtained from experiment and derived model shows low deviations on the part of the model-predicted values relative to values obtained from the experiment. This was attributed to the fact that the surface properties of clay and the physico-chemical interactions between the clay and the binder which played vital roles during water absorption were not considered during the model formulation. This necessitated the introduction of correction factor, to bring the model-predicted apparent porosity to those of the corresponding experimental values.

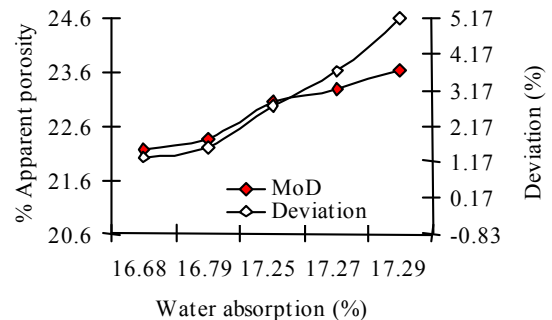


Fig. 8: Variation of deviation with apparent porosity (relative to WAL)

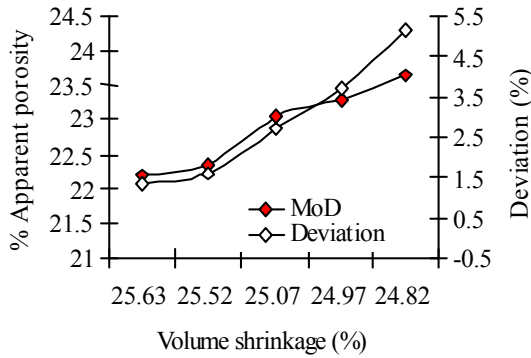


Fig. 9: Variation of deviation with apparent porosity (relative to PFVS)

Deviational analysis from Figs. 8 and 9 indicates that the precise maximum deviation of model-predicted AP from the experimental results is 5.16%. This translated into over 94% operational confidence for the derived model as well as over 0.94 effective coefficients for the functional relationship between AP, PFVS and WAL of the submerged ceramic during service.

Consideration of equation (9) and critical analysis of Figs. 8 and 9 shows that the least and highest magnitudes of deviation of the model-predicted AP (from the corresponding experimental values) are + 1.32 and + 5.16%. Figs. 4, 5, 8 and 9 indicates that these deviations correspond to APs: 22.19 and 23.64 %, PFVSs: 25.63 and 24.82%, as well as WALs: 16.68 and 17.29 % respectively.

Correction factor, Cf to the model-predicted results is given by,

$$Cf = - \left(\frac{\delta_{MoD} - \delta_{ExD}}{\delta_{ExD}} \right) \times 100 \quad (10)$$

Critical analysis of Figs. 8, 9 and Table 6 indicates that the evaluated correction factors are negative of the deviation as shown in equations (9) and (10).

The correction factor took care of the negligence of operational contributions of the surface properties of the clay and the physico-chemical interactions between the clay and the binder which actually played vital role during the water absorption process. The model predicted results deviated from those of the experiment because these contributions were not considered during the model formulation. Introduction of the corresponding values of Cf from equation (10) into the model gives exactly the corresponding experimental values of the apparent porosity.

Table 6: Correction factor to model-predicted apparent porosity

(θ)	(ξ)	Cf (%)
25.63	21.90	- 1.32
25.52	22.01	- 1.59
25.07	22.44	- 2.72
24.97	22.46	- 3.70
24.82	22.48	- 5.16

Table 6 also shows that the least and highest correction factor (to the model-predicted water absorption) are - 1.32 and - 5.16 %. Since correction factor is the negative of deviation as shown in equations (9) and (10), Table 6, Figs. 8 and 9 indicate that these highlighted correction factors corresponds to APs: 22.19 and 23.64 %, PFVSs: 25.63 and 24.82%, as well as WALs: 16.68 and 17.29 % respectively.

It is important to state that the deviation of model predicted results from that of the experiment is just the magnitude of the value. The associated sign preceding the value signifies that the deviation is a deficit (negative sign) or surplus (positive sign).

CONCLUSION

Following analysis of the AP of submerged bricks during service condition, it was concluded that there is increase in AP as PFVS decreases, culminating to increase in WAL. The validity of the derived model was rooted in the core expression $\xi - 102.3089 = - 0.9501 \xi - 2.5076 \theta$ where both side of the expression are correspondingly approximately equal. Generated results indicated that the correlations between AP, WAL and PFVS and the standard error incurred in predicting AP for each value of the PFVS & WAL considered, as obtained from experiment, derived model and regression model were all > 0.95 as well as 0.0659, 0.0668 and 0.0031 & 0.0027, 0.2111 and 0.0637 % respectively. The maximum deviation of the model-predicted AP (from experimental results) was less than 6%. This translated into over 94% operational confidence for the derived model as well as over 0.94 effective coefficients for the functional relationship between AP, WAL and PFVS of the submerged bricks.

REFERENCES

1. Barsoum, M., 1997. Fundamentals of Ceramics. McGraw Hill Incorporated, Singapore, pp: 410.
2. Anwar, M.Y., P.F. Messer, H.A. Davies and B. Ellis, 1995. Ceramic Technology International 1996. Sterling Publications Ltd., London, pp: 95-96, 98.
3. Odriozola, A., M. Gutierrez, U. Haupt and A. Centeno, 1996. "Injection Moulding of Porcelain Pieces" Bol. Soc. Esp. Ceram. Vidrio, 35(2):103-107.

4. Haupt, U., 1998. Injection Moulding of Cups with Handles. *International Ceramics*, 2:48-51.
5. Haupt, U., 2003. Injection Moulding Technology in Table ware Production. *Ceramics World Review*, 13(54): 94, 96-97.
6. Rado, P., 1969. *An Introduction to the Technology of Pottery*. Pergamon Press.
7. Fortuna, D., 2000. 'Sanitary ware Technology' Gruppo Editoriale Faenza Editrice S. p.A.
8. Viewey, F. and P. Larrly, 1978. *Ceramic Processing Before Firing*, John-Wiley and Sons, New York, pp: 3-8.
9. Reed, J., 1988. *Principles of Ceramic Processing*, Wiley Inter science Publication, Canada, pp: 470-478.
10. Keey, R.B., 1978. *Introduction to Industrial Drying Operations*, Pergamon Press, Elmsford, New York, pp: 132-157.
11. Nwoye, C.I., 2008. Mathematical Model for Computational Analysis of Volume Shrinkage Resulting from Initial Air- Drying of Wet Clay Products. *Int. Res. J. Eng. Sc. & Tech.*, 5(1): 82-85.
12. Nwoye, C.I., I.O. Iheanacho and O.O. Onyemaobi, 2008. Model for the Evaluation of Overall Volume Shrinkage in Molded Clay Products from Initial Air-Drying Stage to Completion of Firing. *Int. J. Nat. Appl. Sc.*, 4(2): 234-238.
13. Nwoye, C.I., E.O. Obidiegwu and C.N. Mbah, 2014. Production of Bricks for Building Construction and Predictability of Its Post Fired Volume Shrinkage Based on Apparent Porosity and Water Absorption Capacity. *Research and Reviews: Journal of Materials Science*, 2(3): 17-26.
14. BS EN ISO 10545-3: 1997.
15. Nwoye, C.I., 2008. C-NIKBRAN Data Analytical Memory - Software.